Quantification of Target Engagement of PD-L1 Therapeutics with PET

Dhiraj Kumar[#1], Ala Lisok[#1], Elyes Dahmane[2], Matthew McCoy[3], Sagar Shelake[1], Samit Chatterjee[1], Viola Allaj[4], Polina Sysa-Shah[1], Bryan Wharram[1], Wojciech G. Lesniak[1], Ellen Tully[5], Edward Gabrielson[5,6], Elizabeth M. Jaffee[6], John T. Poirier[4], Charles M. Rudin[4], Jogarao V.S. Gobburu[2], Martin G. Pomper[1,6,7], Sridhar Nimmagadda[1,6,7,8*]

[1]The Russell H. Morgan Department of Radiology and Radiological Science, The Johns Hopkins University School of Medicine, Baltimore, MD, 21287, USA.
[2]Center for Translational Medicine, University of Maryland, Baltimore, MD, 21201, USA.
[3]Innovation Center for Biomedical Informatics, Georgetown University, Washington, DC, 20007,USA.
[4]Department of Medicine, Memorial Sloan Kettering Cancer Center, New York, NY, 10065, USA.
[5]The Department of Pathology, The Johns Hopkins University School of Medicine, Baltimore, MD, 21287, USA.
[6]The Sidney Kimmel Comprehensive Cancer Center, Johns Hopkins University School of Medicine, Baltimore, MD, 21287, USA.
[7]Pharmacology and Molecular Sciences, Johns Hopkins University School of Medicine, Baltimore, MD, 21287, USA.
[8]Division of Clinical Pharmacology, Department of Medicine, Johns Hopkins University School of Medicine, Baltimore, MD, 21287, USA.

*Correspondence to: Sridhar Nimmagadda, Ph.D.
Johns Hopkins Medical Institutions
1550 Orleans Street, CRB II, #491
Baltimore, MD 21287
Phone: 410-502-6244
Fax: 410-614-3147
Email: snimmag1@jhmi.edu

#, equal contribution

LIST of SUPPLEMENTARY MATERIALS

Supplementary Figure 1A. WL12 binding interface on PD-L1.

Supplementary Figure 2A. Characterization of Cy5 conjugated antibodies.

Supplementary Figure 2B. PD-L1 expression in cell lines.

Supplementary Figure 2C and D. WL12 inhibits antibody binding to PD-L1.

Supplementary Figure 2E. PD-1:PD-L1 blockade functional assay response to PD-L1 inhibition by AtzMab and WL12.

Supplementary Figure 2F. Mutations in PD-L1 in human tumors in cBioportal.

Supplementary Figure 2G. Mutations in PD-L1 in cell lines in CCLE database.

Supplementary Figure 2H. Known PD-L1 cell line variants.

Supplementary Figure 2I. [^{64}Cu]WL12 binding in HCC1569 cell line with M115T mutation.

Supplementary Figure 3. Ex vivo biodistribution of [^{64}Cu]WL12 in mice bearing H226 (B), HCC827 (C) or hPD-L1/CHO (D) tumors following AtzMab treatment.

Supplementary Figure 4. Ex vivo biodistribution of [^{64}Cu]WL12 in mice bearing A549/A549-iPDL1 tumors following AtzMab treatment.

Supplementary Figure 5A. Ex vivo biodistribution of [^{64}Cu]WL12 in mice bearing MDAMB231 tumors following AtzMab, AveMab and DurMab treatment.

Supplementary Figure 5B. Western blot analysis of PD-L1 expression in MDAMB231 and SUM149 cells treated with PD-L1 antibodies.

Supplementary Figure 6. *Ex vivo* biodistribution of [^{64}Cu]WL12 in MDAMB231tumor bearing mice treated with escalating dose of AtzMab.

Supplementary Figure 1. A representation of the molecular surface surrounding the PD-L1 interaction interface with PD-1 and PD-L1 inhibitors. The common residues involved in interactions with PD-1 competitive therapeutics is shown in cyan, the molecular contacts specific to the PD-1 interactions are shown in purple, and non-interacting residues are shown in grey. To illustrate the overlap in molecular interaction, the structure of bound PD-1 is shown in purple and the predicted conformation of WL12 is shown in green. WL12 binding mode to PD-L1 overlaps those of PD-1, AtzMab, AveMab, DurMab, BMS936559 and KM035.

Supplementary Figure 2. **A,** Characterization of Cy5 conjugated antibodies by nanodrop and MALDI-TOF. **B**, PD-L1 expression in various cell lines and the corresponding mean fluorescence intensity values. **C**, WL12 (5 nM) inhibits binding of Cy5-conjugated- AtzMab, AveMab and DurMab (2 nM) to PD-L1 in hPD-L1, MDAMB231, HCC827 and H226 cells. **D**, Mean fluorescence intensity determined by flow cytometry. **E**, PD-1:PD-L1 blockade functional assay response to PD-L1 inhibition by AtzMab and WL12. **F**, Mutations in PD-L1 in human tumors. **G**, Mutations in PD-L1 in cell lines in CCLE database. **H**, The locations of residues mutated in PD-L1 expressing cell lines (red) from figure 2F. **I,** PD-L1 expression and [^{64}Cu]WL12 binding to H1569 cells with M115T mutation. Uptake assay was performed as described in the methods section. ****, P<0.0001 by unpaired t-test in D.

Supplementary Figure 3. **A,** WL12-DOTAGA radiolabeling conditions and radiochemical purity of [^{64}Cu]WL12-DOTAGA. **B-D,** *Ex vivo* biodistribution of [^{64}Cu]WL12 in mice bearing H226 (B), HCC827 (C) or hPD-L1/CHO (D) tumors. Mice were treated with 20 mg/Kg dose of AtzMab 24h prior to tracer injection. Data shown is mean±SEM (n=8-12/group). ****, P<0.0001; ***, P<0.001; NS, not significant, by unpaired t-test.

Supplementary Figure 4. **A,** *Ex vivo* biodistribution of [^{64}Cu]WL12 in A549-iPDL1 and A549 control tumor bearing mice given doxycycline for 72h and treated with 20mg/Kg of AtzMab 24 h prior to radiotracer injection. Data shown is mean±SEM (n=10/group). ****, P<0.0001; NS, not significant, by 1-way ANOVA and Sidak's multiple comparisons test.

Supplementary Figure 5. **A,** *Ex vivo* biodistribution of [^{64}Cu]WL12 in MDAMB231 bearing mice treated with AtzMab (20mg/Kg), AveMab (10 mg/Kg), or DurMab (10 mg/Kg) for 24 h prior to radiotracer injection. Biodistribution was performed at 2h after [^{64}Cu]WL12 injection (mean±SEM; n=6-9/group). **B**, western blot analysis of PD-L1 in MDAMB231 and SUM149 cells treated with AtzMab, AveMab and DurMab at 6 μg/mL for 72h. ****, P<0.0001; NS, not significant, by 1-way ANOVA and Dunnett's multiple comparisons test.

Supplementary Figure 6. **A,** *Ex vivo* biodistribution of [^{64}Cu]WL12 in MDAMB231 tumor bearing mice treated with escalating dose of AtzMab (0.0009 to 12 mg/Kg) 24h prior to tracer injection. Biodistribution was performed at 2h after [^{64}Cu]WL12 injection. Data are mean±SEM (n=3-7/group).

METHODS AND RESULTS.

The PD-L1/PD-1 blockade functional bioassay.

The PD-L1/PD-1 blockade functional bioassay was performed using the Promega kit (Catalog #CS187111, Promega) as per the manufacturer's protocol. Briefly, 40000 PD-L1 aAPC/CHO-K1 cells/well in 100μL F12 medium with 10% FBS were plated in 96 well B&W iso-plate (PerkinElmer, #6005060) and incubated over-night at 37^{o}C. Next day, the medium was

removed and peptide dilutions (concentration range: 10^{-5} M to 10^{-13} M) in 40µL RPMI with 1% FBS were added to each well. Then, 40000 PD-1 Effector cells (Jurkat T cells expressing human PD-1 and a luciferase reporter driven by an NFAT response element) in 40µL RPMI with 1% FBS were added to each well and co-cultured at 37ºC. After 6h, 80 µL Bio-Glo™ reagent was added, incubated for 20 min at room temperature and the bioluminescence was measured in VICTOR3V 1420 Multilabel Counter (PerkinElmer) with 0.5s integration time. Data were analyzed in GraphPad Prism 6 software.

In whole cell functional assays EC_{50} values of 23.6 nM (95% CI 21.4-26.1 nM) and 1.72 nM (95% CI 1.16-2.53 nM) were observed for WL12 and AtzMab, respectively (Supplementary figure 2E), indicating that WL12 peptide inhibits PD-1:PD-L1 interaction and at a 10 fold lower potency than AtzMab.

Analysis of effect of PD-L1 antibody treatment on PD-L1 expression in cell lines by western blot.

To study the effect of PD-L1 antibody treatment on PD-L1 expression in cancer cells, MDAMB231 (1 million) and SUM149 (1.5 million) cells were seeded in 10 cm^2 cell culture dish and treated with 6 µg/mL of AtzMab, AveMab or DurMab for 72 h and assessed for PD-L1 protein expression in whole cell lysate using western blot analysis. Antibody treated cells were washed twice with ice cold PBS and whole cell lysates were prepared using RIPA buffer as per the standard protocol (Sigma # R0278) supplemented with protease inhibitor cocktail. Protein quantification was performed using Pierce™ BCA Protein Assay Kit (#23227). Protein extracts (30 µg protein) were boiled with loading buffer containing 2-mercaptoethanol, separated using 10%SDS-polyacrylamide gels, and transferred to nitrocellulose membranes. Blots were blocked with blocking buffer [5% (w/v) nonfat dry milk in 10 mmol/L Tris (pH

7.5), 10 mmol/l sodium chloride, and 0.1% Tween 20 (TBST)] for 30–60 min at room temperature. Blots were incubated with the primary antibodies, anti-hPD-L1 rabbit (Cell Signaling Technology # 13684T) and anti-hActin rabbit (Santa Cruz # C2009) overnight at 4 °C. The antibody labeled blots were washed three times with 1X TBST for 15 min each and incubated with 1:5000 dilution of horse-radishperoxidase conjugated secondary antibody for 1h at 4 °C. Membranes were developed with ECL reagent as Pierce™ ECL Western Blotting Substrate (#32106) and Hyblot Cl autoradiography film (Denville Scientific # E3018).

Effect of IFNγ on PD-L 1 expression by flow cytometry.

Effect of IFN gamma treatment on PD-L1 expression was assed using flow cytometry. HCC1569 cells were seeded in 6 well cell culture plate and treated with 200 ng/mL of recombinant hIFNγ (Biotechne, #AFL285) for 24 h. Cells were washed twice with 1X HBSS and PD-L1 expression was analyzed by flow cytometry as per the described protocol in this manuscript.

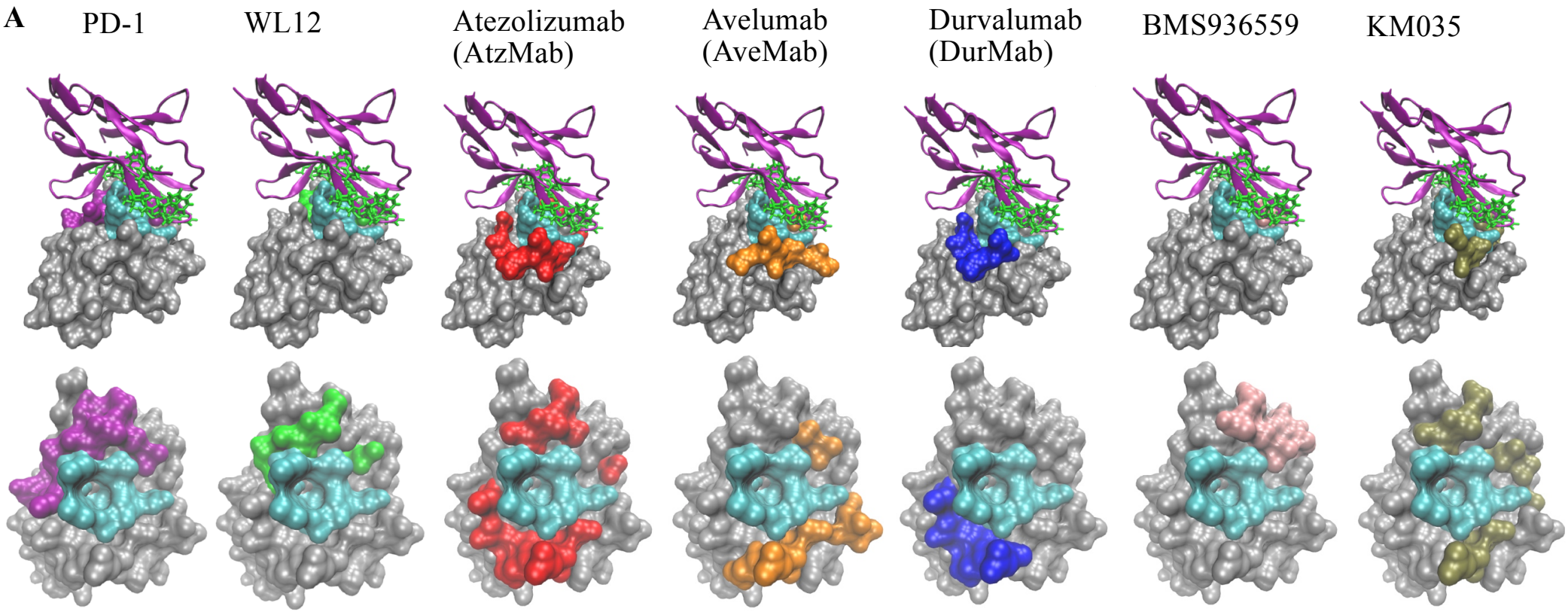

Supplementary Figure 1: **A representation of the molecular surface surrounding the PD-L1 interaction interface with PD-1 and PD-L1 inhibitors.** The common residues involved in interactions with PD-1 competitive therapeutics is shown in cyan, the molecular contacts specific to the PD-1 interactions are shown in purple, and non-interacting residues are shown in grey. To illustrate the overlap in molecular interaction, the structure of bound PD-1 is shown in purple and the predicted conformation of WL12 is shown in green. WL12 binding mode to PD-L1 overlaps those of PD-1, other reported peptides, AtzMab, AveMab, DurMab, BMS936559 and KM035.

Supplementary Figure 2A

Cy5 NHS labeled Antibody characterization by UV-Vis Spectroscopy (Nanodrop)

Antibody (Ab)	A280	Ab Conc. [M]	A650	Cy5-Ab Conc [M]	Cy5-NHS : Ab
AtzMab	0.187	8.9E-08	0.537	2.1E-07	2.41
AveMab	0.308	1.5E-07	0.845	3.4E-07	2.30
DurMab	0.313	1.5E-07	0.922	3.7E-07	2.47

A=eCl ; where
A= Absorbance max, e= molar extinction coefficient and **l**=pathlength
e =250 000 $M^{-1}cm^{-1}$ at 650 nm for the cy5 dye (Refer: GE healthcare catalogue product PA15101)
ε =170 000 $M^{-1}cm^{-1}$ at 280 nm for the antibody

Supplementary Figure 2. A, Characterization of Cy5 conjugated antibodies by nanodrop and MALDI-TOF. **B**, PD-L1 expression in various cell lines and the corresponding mean fluorescence intensity values. **C**, WL12 (5 nM) inhibits binding of Cy5-conjugated- AtzMab, AveMab and DurMab (2 nM) to PD-L1 in hPD-L1, MDAMB231, HCC827 and H226 cells. **D**, Mean fluorescence intensity determined by flow cytometry. **E**, PD-1:PD-L1 blockade functional assay response to PD-L1 inhibition by AtzMab and WL12. **F**, Mutations in PD-L1 in human tumors. **G**, Mutations in PD-L1 in cell lines in CCLE database. **H**, The locations of residues mutated in PD-L1 expressing cell lines (red) from figure 2F. Of the five variants in the PD-L1 binding domain, only M115T is part of the common core of PD-L1 binding residues (cyan). Left and right panels show a rotated view of the PD-L1 domain. **I,** PD-L1 expression and [^{64}Cu]WL12 binding to H1569 cells with M115T mutation. Uptake assay was performed as described in the methods section. ****, P<0.0001 by unpaired t-test in D.

Supplementary Figure 2A

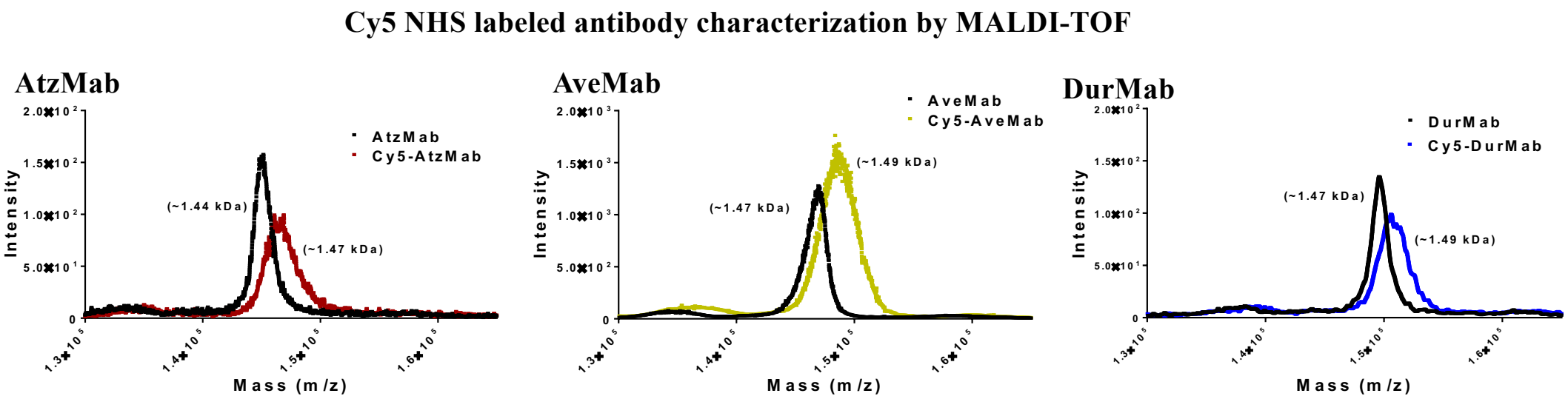

Supplementary Figure 2A

MALDI-TOF characterization of Atezolizumab

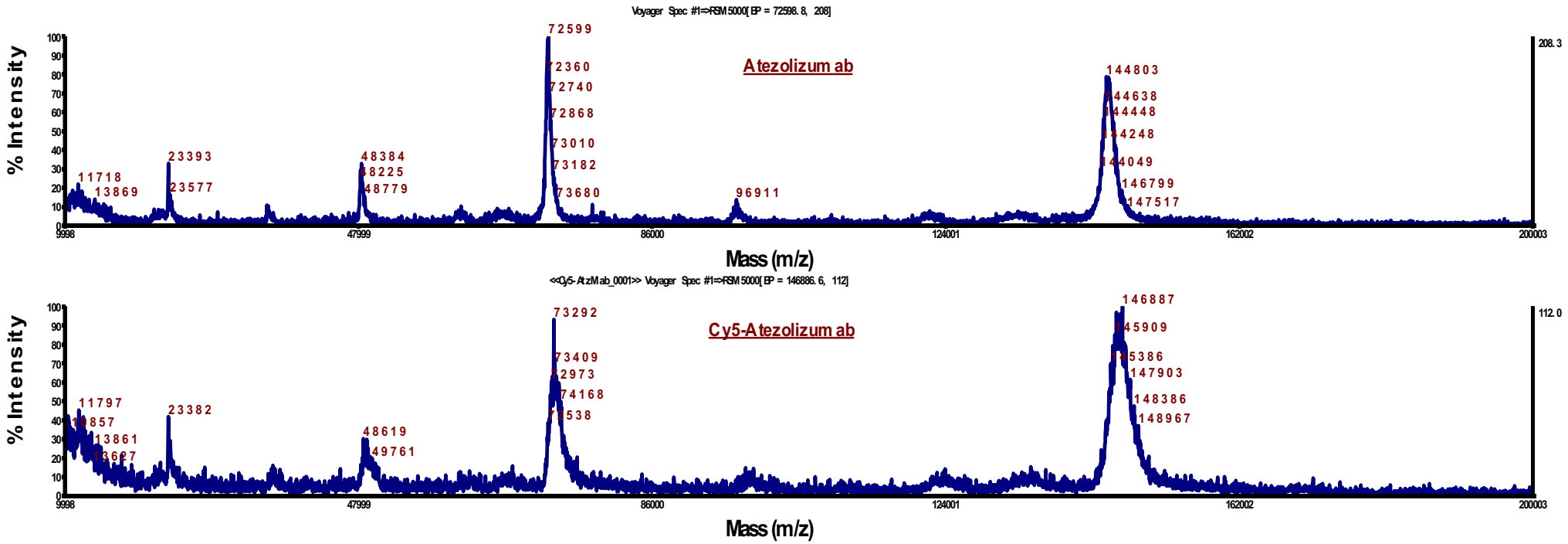

Supplementary Figure 2A

MALDI-TOF characterization of Avelumab

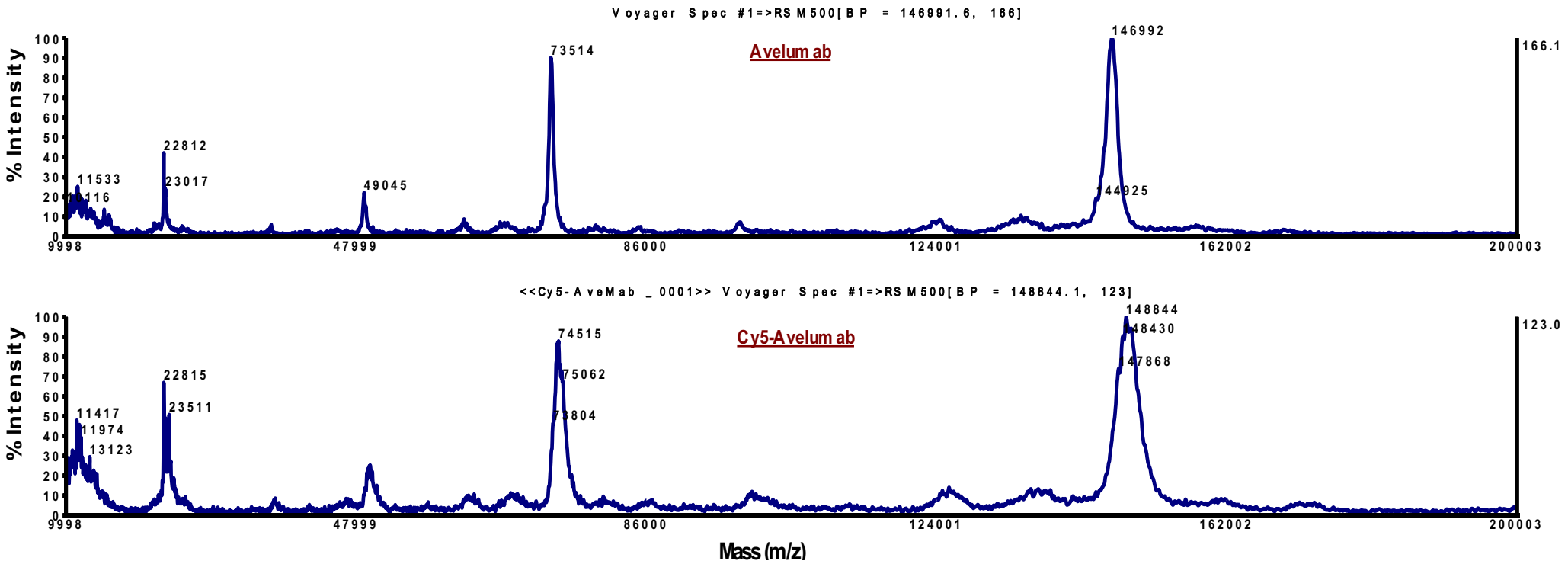

Supplementary Figure 2A

MALDI-TOF characterization of Durvalumab

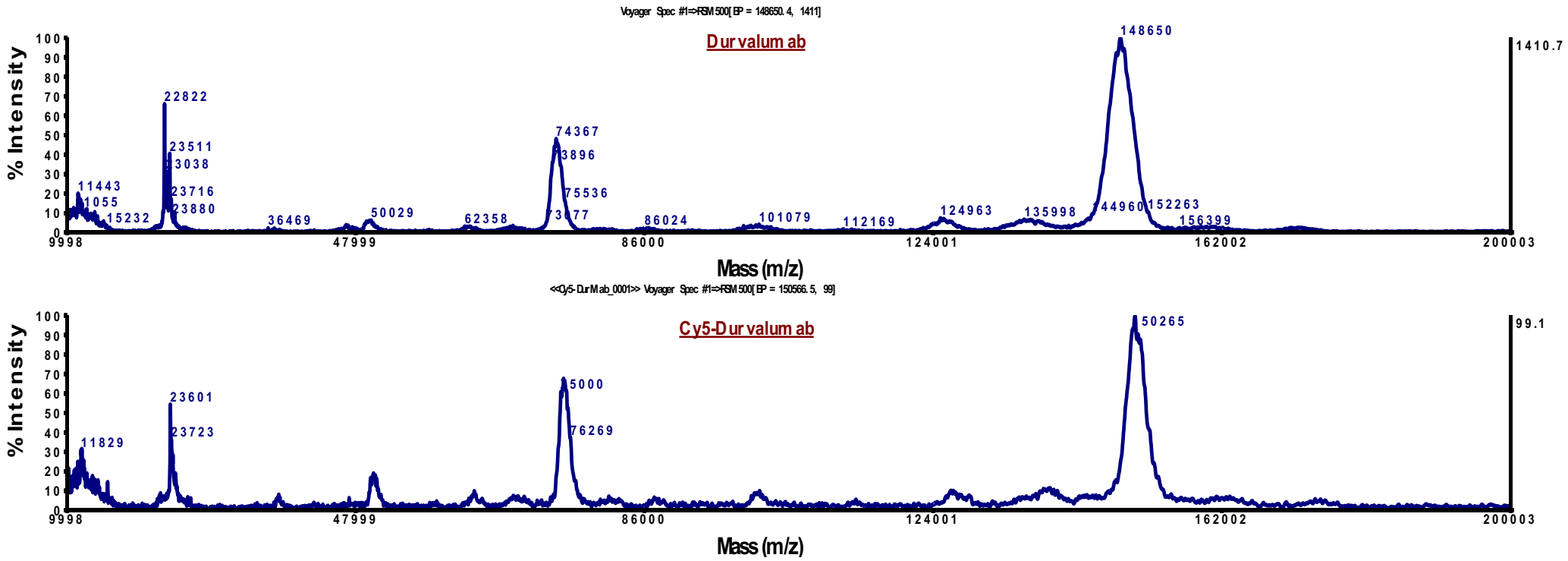

Supplementary Figure 2B

B

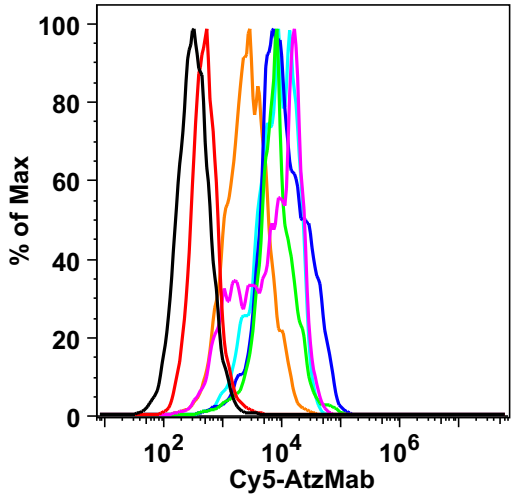

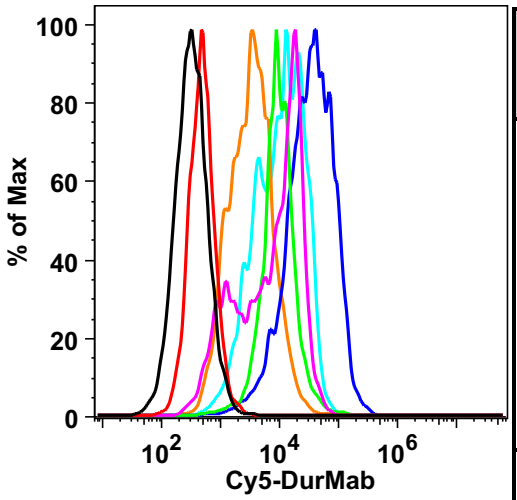

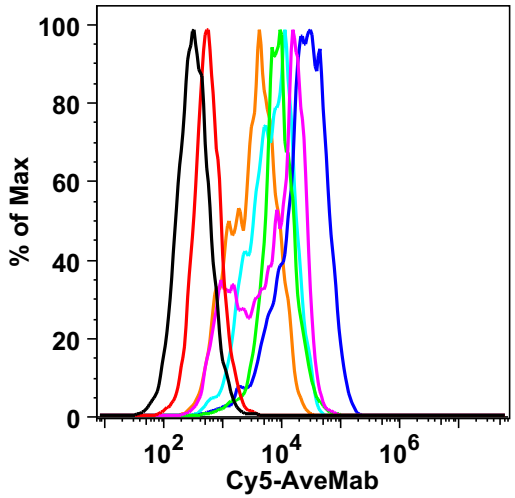

Antibody	Sample	MFI	SEM
Cy5-AtzMab	Unstained	369	30
	A549-iPDL1	5831	28
	CHOK1-PDL1	10906	55
	MDAMB231	7471	232
	H226	2539	47
	HCC827	7722	168
Cy5-AveMab	A549-iPDL1	6250	95
	CHOK1-PDL1	22309	1156
	MDAMB231	8577	169
	H226	3156	63
	HCC827	5742	376
Cy5-DurMab	A549-iPDL1	6125	72
	CHOK1-PDL1	33642	2426
	MDAMB231	9329	495
	H226	3242	5
	HCC827	7763	1045

Supplementary Figure 2C & D

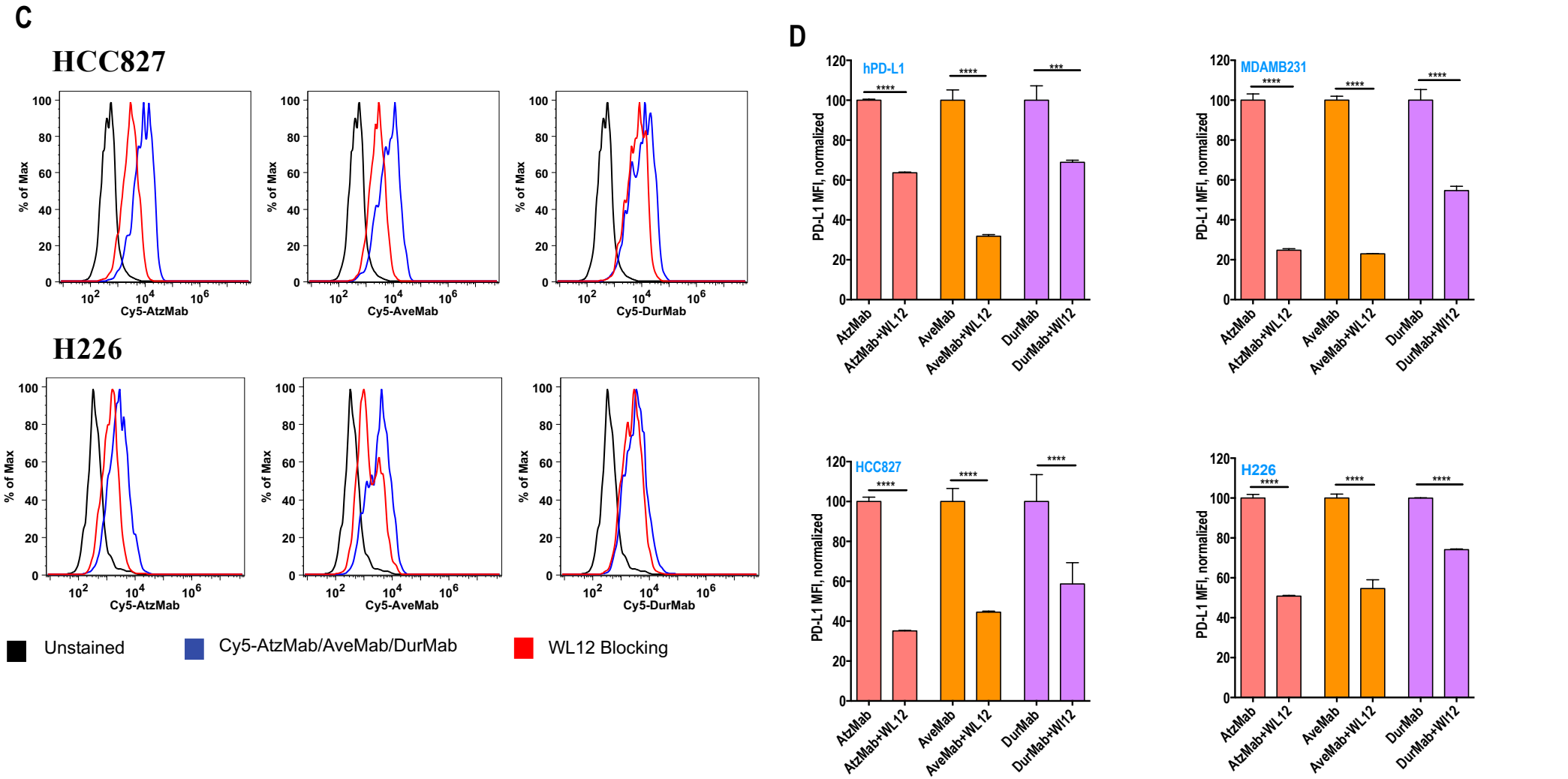

Supplementary Figure 2E

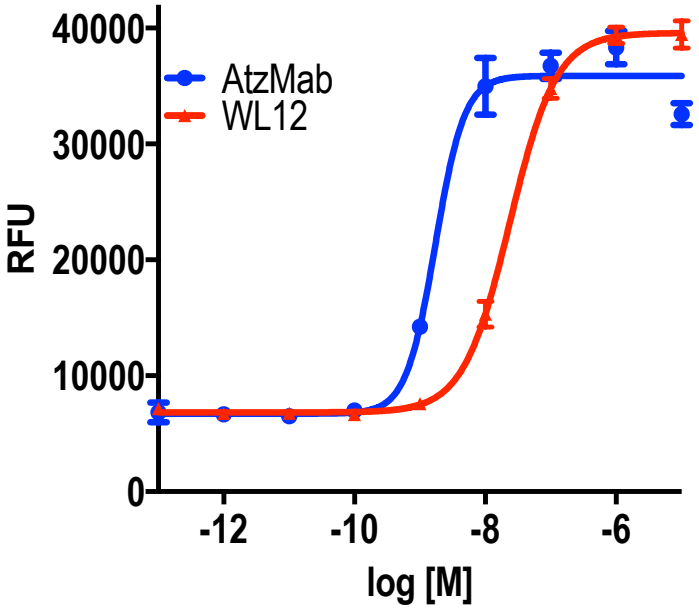

	AtzMab	WL12
IC_{50}	1.72e-009	2.364e-008
95% CI	1.167e-009 to 2.534e-009	2.142e-008 to 2.611e-008

Supplementary Figure 2F

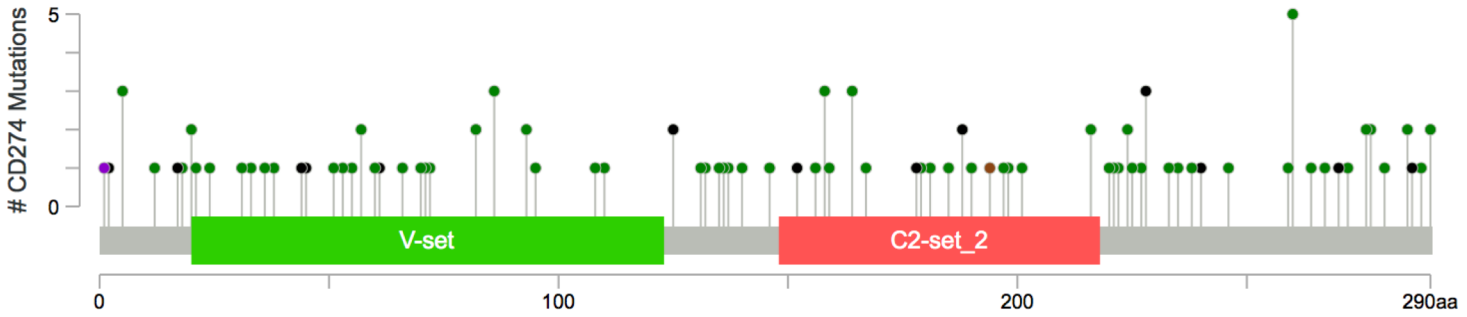

CD274
UniProt: PD1L1_HUMAN
Transcript: ENST00000381577
Somatic Mutation Frequency:0.2%
135 Missense
24 Truncating
2 Inframe
7 Other

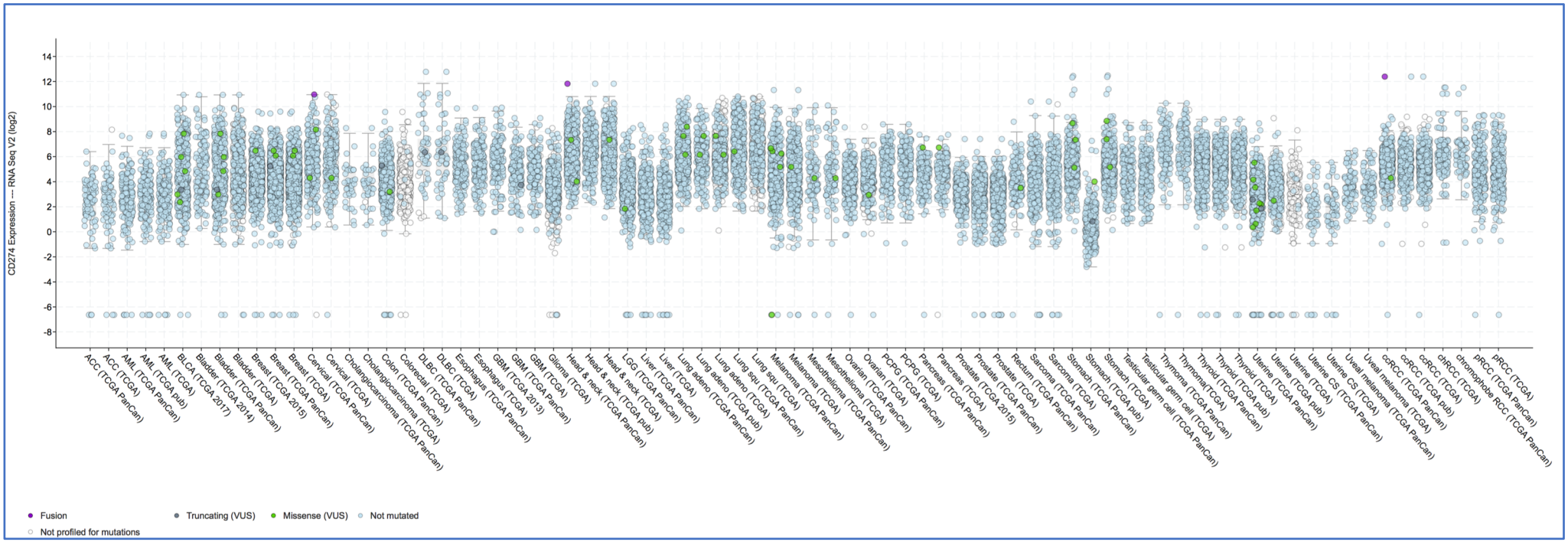

Supplementary Figure 2G

Hugo Symbol	Entrez Gene Id	Tumor Sample Barcode	Ncbi Build	Chr	Start Position	End Position	Variant Classification	Variant Type	Reference Allele	Tumor Seq Allele	dbSNP ID	Annotation Transcript	Protein Change
CD274	29126	AMO1_HAEMATOPOIETIC_AN	37	9	5462893	5462893	Nonsense_Mutati	SNP	G	T	NA	ENST00000381577.3	p.E152*
CD274	29126	CI1_HAEMATOPOIETIC_AND_L	37	9	5456116	5456116	Start_Codon_SNP	SNP	G	T	NA	ENST00000381577.3	p.M1I
CD274	29126	DMS454_LUNG	37	9	5463102	5463102	Silent	SNP	A	T	NA	ENST00000381577.3	p.T221T
CD274	29126	HEC108_ENDOMETRIUM	37	9	5457184	5457184	Missense_Mutati	SNP	T	C	NA	ENST00000381577.3	p.L53P
CD274	29126	SNU520_STOMACH	37	9	5456164	5456164	Splice_Site	SNP	C	T	NA	ENST00000381577.3	p.N17N
CD274	29126	TOV21G_OVARY	37	9	5457316	5457316	Missense_Mutati	SNP	C	T	NA	ENST00000381577.3	p.A97V
CD274	29126	NCIH2171_LUNG	37	9	5466801	5466801	Silent	SNP	C	T	NA	ENST00000381577.3	p.I274I
CD274	29126	HCC1569_BREAST	37	9	5457370	5457370	Missense_Mutati	SNP	T	C	NA	ENST00000381577.3	p.M115T
CD274	29126	JHH7_LIVER	37	9	5457282	5457282	Missense_Mutati	SNP	C	T	NA	ENST00000381577.3	p.R86W
CD274	29126	MFE319_ENDOMETRIUM	37	9	5465606	5465606	Splice_Site	SNP	G	T	NA	ENST00000381577.3	p.G264W
CD274	29126	SCABER_URINARY_TRACT	37	9	5465498	5465498	Splice_Site	SNP	G	C	NA	ENST00000381577.3	
CD274	29126	D542MG_CENTRAL_NERVOUS	37	9	5462908	5462908	Missense_Mutati	SNP	G	A	NA	ENST00000381577.3	p.A157T
CD274	29126	HEC1_ENDOMETRIUM	37	9	5462999	5462999	Missense_Mutati	SNP	A	T	NA	ENST00000381577.3	p.E187V
CD274	29126	KYSE270_OESOPHAGUS	37	9	5462878	5462878	Missense_Mutati	SNP	G	T	NA	ENST00000381577.3	p.V147F
CD274	29126	MCC13_SKIN	37	9	5467856	5467856	Silent	SNP	G	A	NA	ENST00000381577.3	p.E289E
CD274	29126	OC314_OVARY	37	9	5457306	5457306	Missense_Mutati	SNP	C	A	NA	ENST00000381577.3	p.L94M
CD274	29126	OMC1_CERVIX	37	9	5467854	5467854	Missense_Mutati	SNP	G	A	NA	ENST00000381577.3	p.E289K
CD274	29126	SNU1040_LARGE_INTESTINE	37	9	5457230	5457230	Silent	SNP	G	A	NA	ENST00000381577.3	p.V68V
CD274	29126	HMEL_BREAST	37	9	5465572	5465572	Silent	SNP	T	C	NA	ENST00000381577.3	p.G252G
CD274	29126	HS739T_BREAST	37	9	5463099	5463099	Silent	SNP	T	C	NA	ENST00000381577.3	p.H220H
CD274	29126	NCIH2347_LUNG	37	9	5465590	5465590	Silent	SNP	C	T	NA	ENST00000381577.3	p.I258I

Supplementary Figure 2H

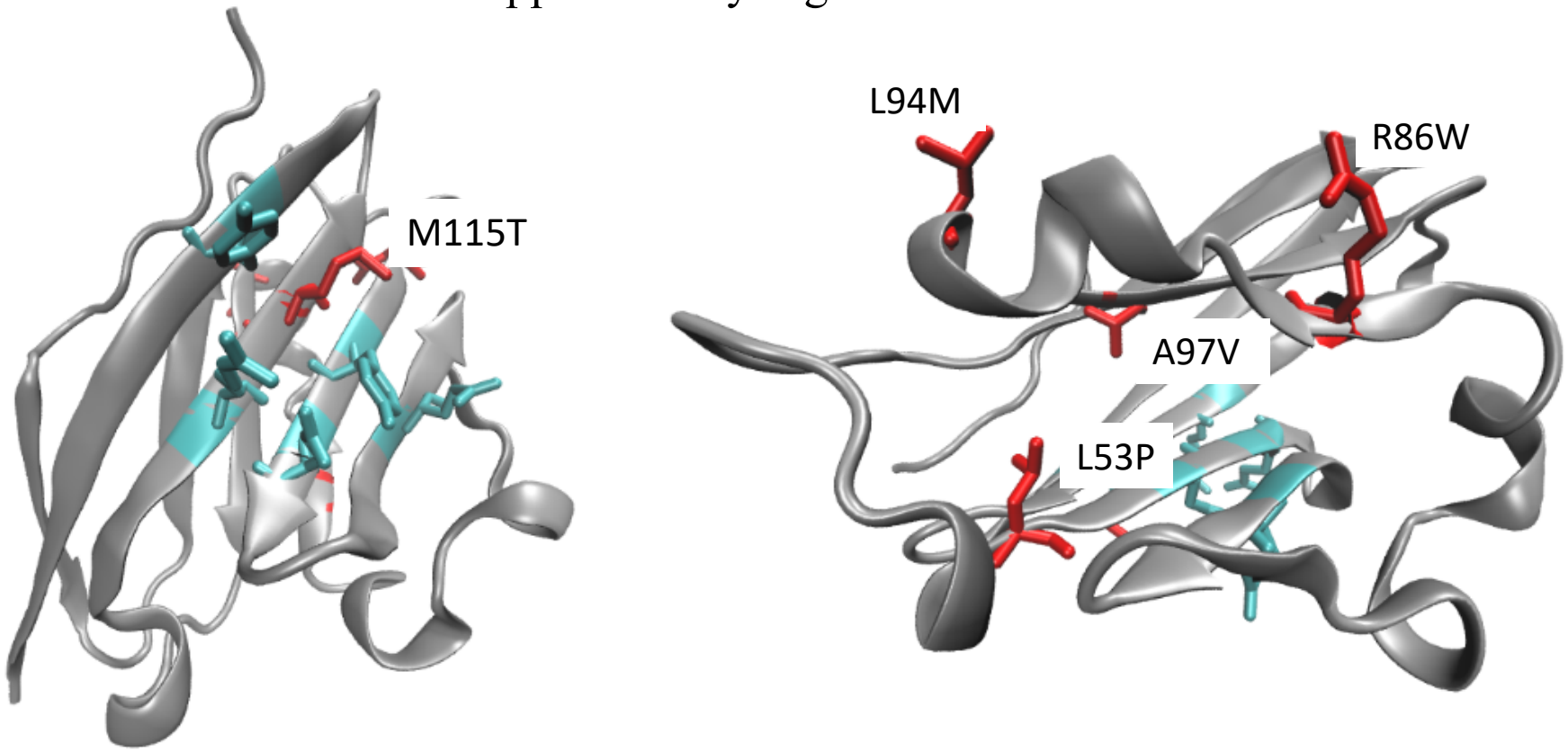

Supplementary Figure 2I

HCC1569 cell line (M115T mutation)

Flow cytometry

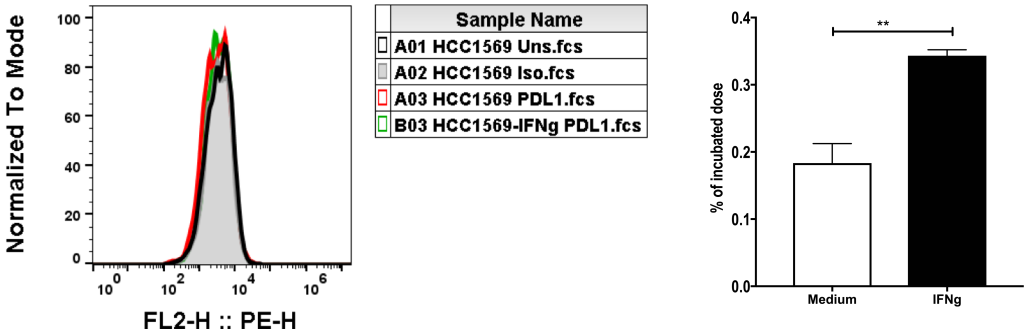

Supplementary Figure 3

A

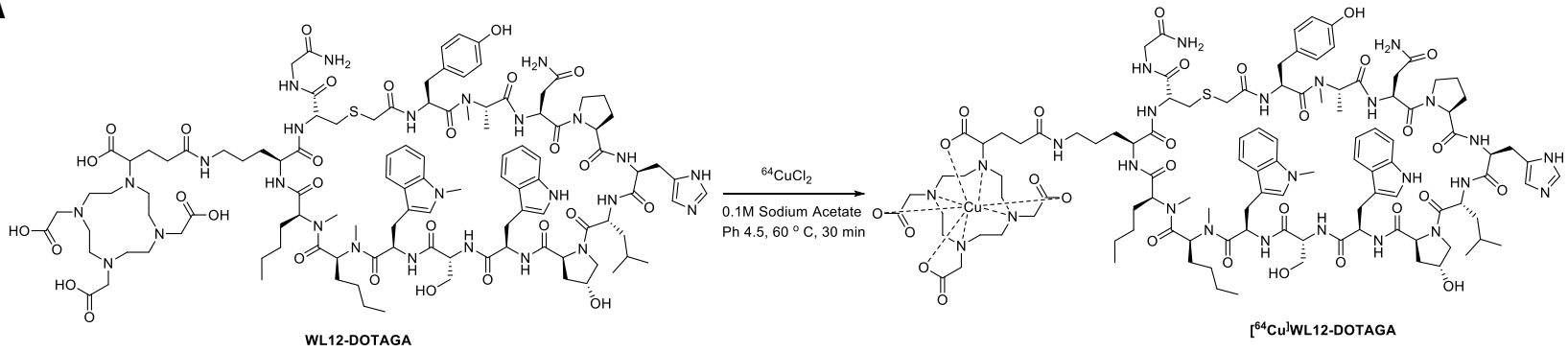

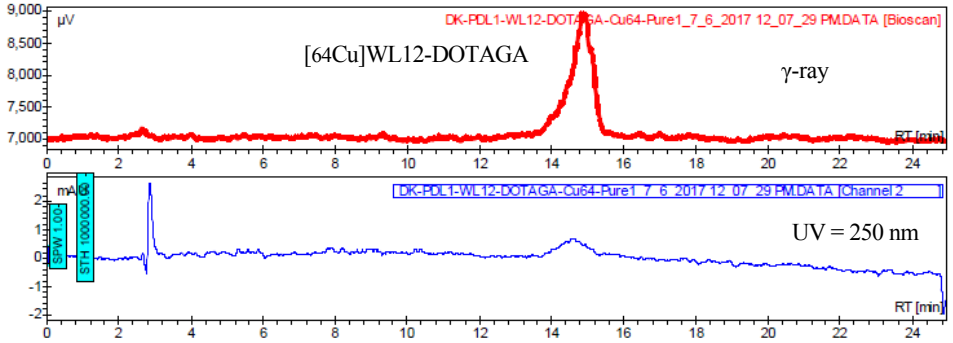

RP-HPLC chromatogram of purified [^{64}Cu]WL12-DOTAGA.

Supplementary Figure 3. A, WL12-DOTAGA radiolabeling conditions and radiochemical purity of [^{64}Cu]WL12-DOTAGA. **B-D,** *Ex vivo* biodistribution of [^{64}Cu]WL12 in mice bearing H226 (B), HCC827 (C) or hPD-L1/CHO (D) tumors. Mice were treated with 20 mg/Kg dose of AtzMab 24h prior to tracer injection (mean±SEM; n=8-12/group) . ****, P<0.0001; ***, P<0.001; NS, , not significant, by unpaired t-test.

Supplementary Figure 3

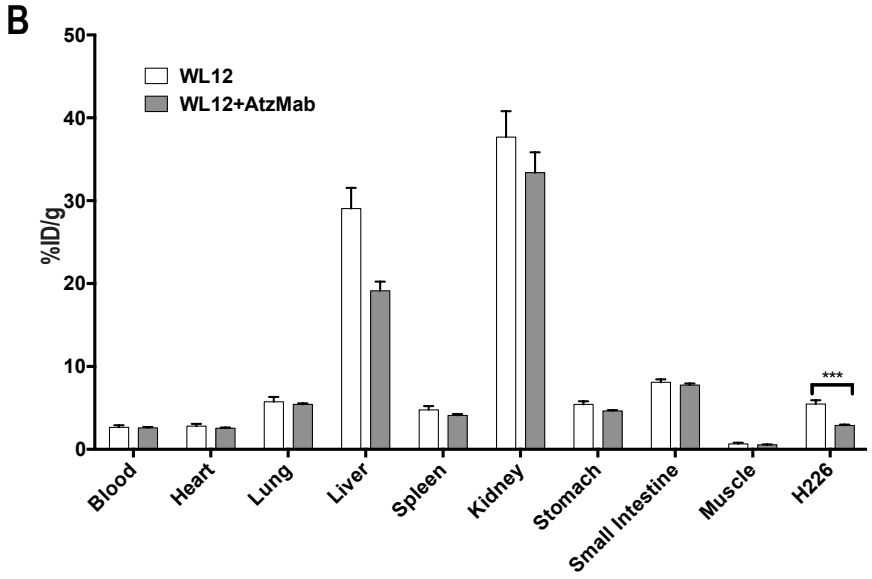

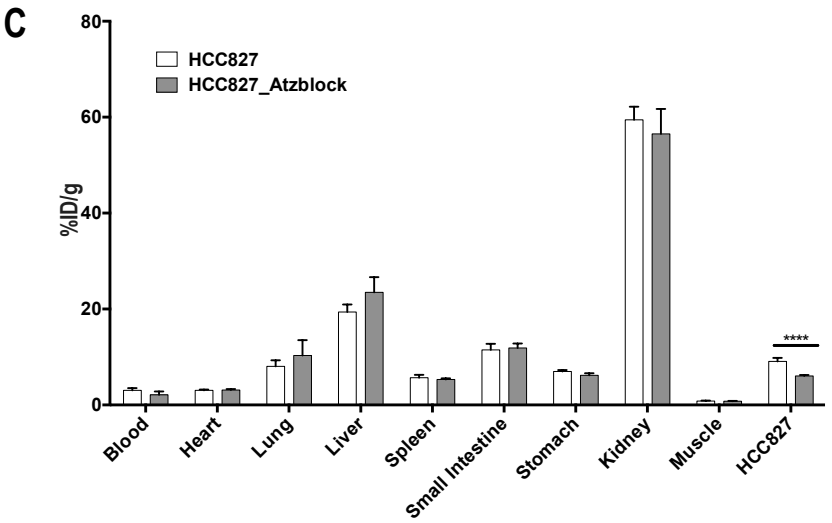

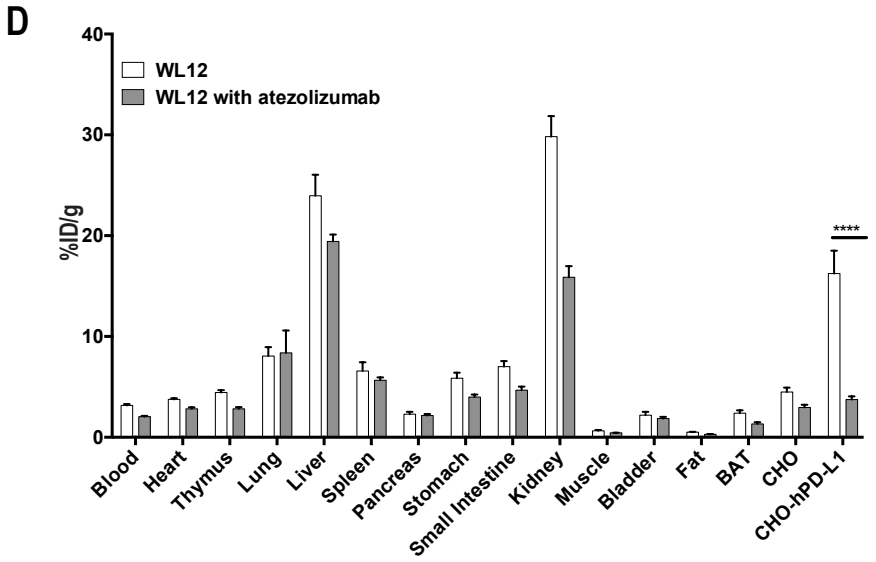

Supplementary Figure 4

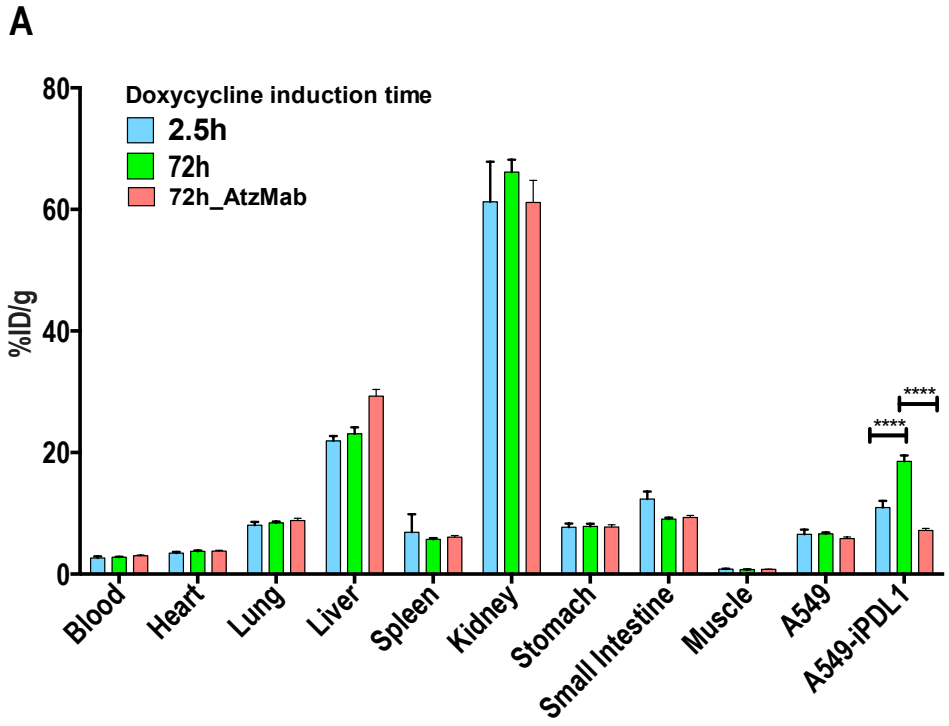

Supplementary Figure 4. A, *Ex vivo* biodistribution of [^{64}Cu]WL12 at 2h after injection in A549-iPDL1 and A549 control tumor bearing mice given doxycycline for 72h and treated with 20mg/Kg of AtzMab 24 h prior to radiotracer injection (mean ± SEM; n=10/group). ****, P<0.0001; NS, not significant, by 1-way ANOVA and Sidak's multiple comparisons test.

Supplementary Figure 5A

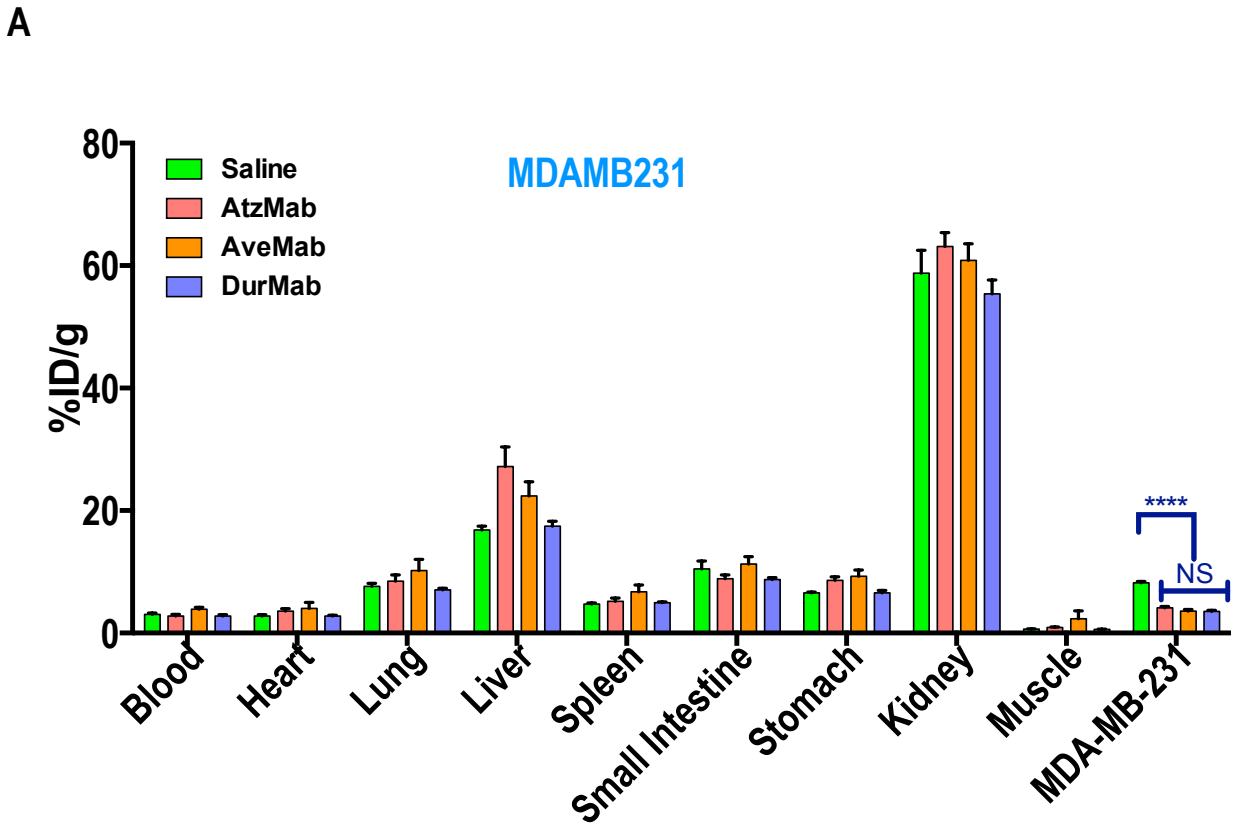

Supplementary Figure 5. A, *Ex vivo* biodistribution of [^{64}Cu]WL12 in MDAMB231 bearing mice treated with AtzMab (20mg/Kg), AveMab (10 mg/Kg), or DurMab (10 mg/Kg) for 24 h prior to radiotracer injection. Biodistribution was performed at 2h after [^{64}Cu]WL12 injection (mean±SEM; n=6-9/group). **B**, western blot analysis of PD-L1 in MDAMB231 and SUM149 cells treated with AtzMab, AveMab and DurMab at 6 µg/mL for 72h. ****, P<0.0001; NS, not significant, by 1-way ANOVA and Dunnett's multiple comparisons test.

Supplementary Figure 5B

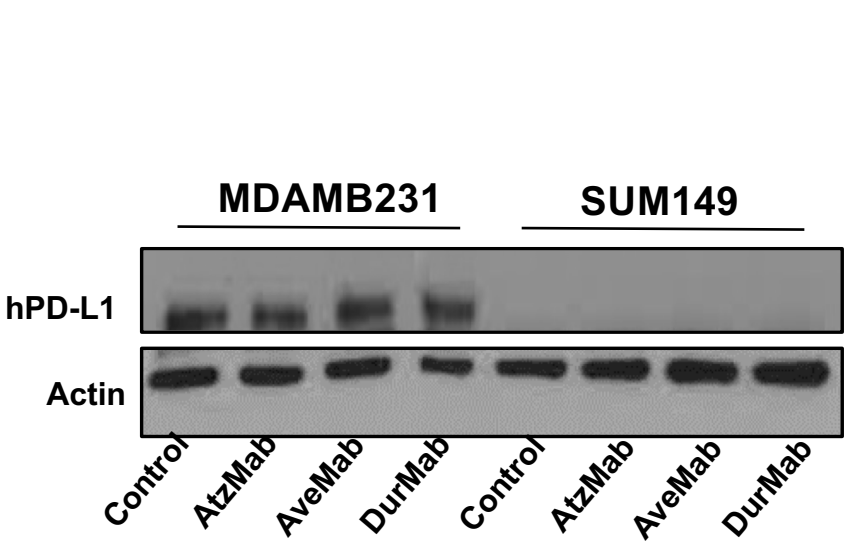

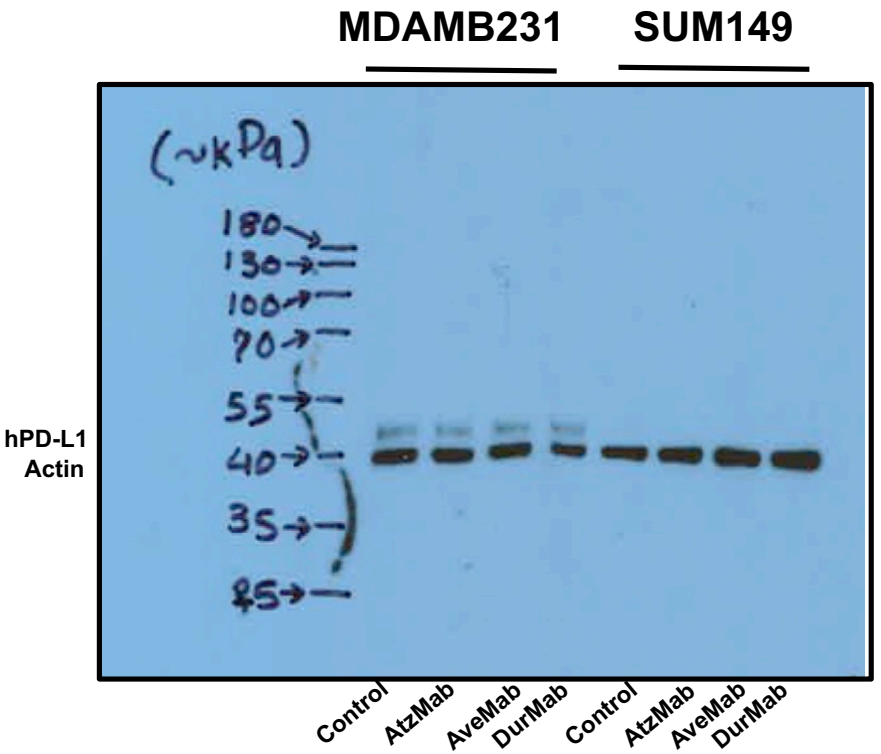

Supplementary Figure 6

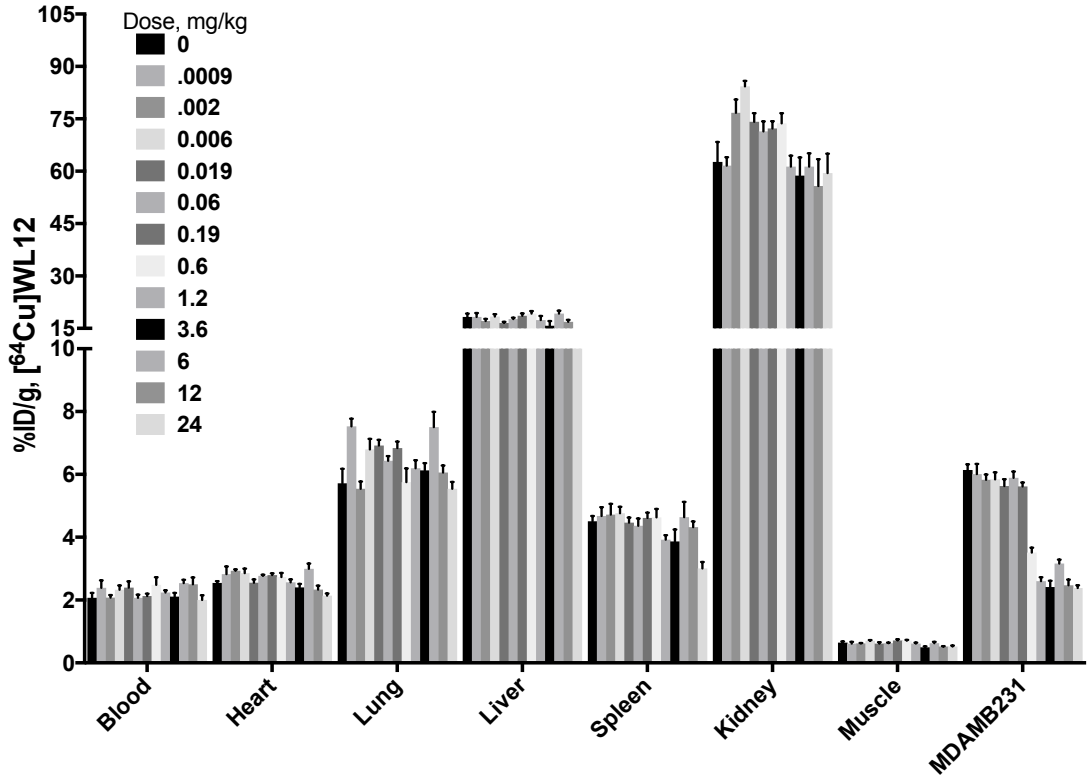

Supplementary Figure 6. A, Ex vivo biodistribution of [^{64}Cu]WL12 in MDAMB231tumor bearing mice treated with escalating dose of AtzMab (0.0009 to 12 mg/Kg) 24h prior to tracer injection. Biodistribution was performed at 2h after [^{64}Cu]WL12 injection. Data are mean ± SEM (n=3-7/group).